Retrofit of RC Frames Using FRP Jacketing or Steel Bracing

T. El-Amoury[1] and A. Ghobarah[2]

1. Department of Civil Engineering, McMaster University, Hamilton, Canada
2. Department of Civil Engineering, McMaster University, Hamilton, Canada, email: ghobara@mcmaster.ca

ABSTRACT: *During recent seismic events, non-ductile failure modes of many existing structures occurred. Retrofit of these structures before the earthquake provides a feasible cost-effective approach to reduce the hazard to occupants' safety and owners' investment. The response of two reinforced concrete frames was examined under seismic excitation. The 9-storey and 18-storey frames are part of the lateral load resisting system in two office buildings that were designed according to the 1960s code provisions. The frames were analyzed assuming flexible joint response by considering the joint shear deformation or assuming traditional rigid joints. Two rehabilitation techniques were proposed to improve the dynamic response of these frames. Fibre reinforced polymer (FRP) jackets were used as a local rehabilitation technique to enhance the joint shear strength and ductility. As another option, X-steel braces were installed in the middle bay of the frame along its height as an alternate lateral load resisting system. For each frame, failure sequence and interstorey drift were examined. It was found that FRP wrapping eliminated the brittle failure modes without significant change in the structural response. However, steel bracing significantly contributed to the structural stiffness and reduced the maximum interstorey drift of the frames.*

Keywords: Seismic; Rehabilitation; Reinforced concrete; Moment resisting frames; FRP; Steel bracing

1. Introduction

Recent earthquakes such as the 1989 Loma Prieta, 1994 Northridge, 1995 Hanshin-Awaji (Kobe) and the 1999 Kocaeli (Turkey) [1] tested the vulnerability of existing reinforced concrete (*RC*) buildings to strong ground motions. Failure of beam-column joints in concrete moment resisting frames was identified as one of the leading causes of collapse of such structures. Therefore, when assessing the response of an existing structure, the conventional rigid joint assumption, which ignores the joint shear deformation and therefore the potential joint shear failure, is invalid. The joint behaviour is governed by the joint shear deformation and the bond behaviour of beam and column reinforcement bars. When the beam reinforcement are well anchored at the beam-column joint, high shear stress is transferred to the joint zone, which requires adequate amount of joint shear reinforcement. On the other hand, if the beam bottom reinforcement were inadequately anchored, bond-slip of the bars would occur which reduces the shear stress transferred to the joint. However, it would result in a fixed end rotation at the beam-joint interface.

Numerous experimental studies were carried out to investigate the behaviour of non-ductile beam-column subassemblies [2-4]. Feasible local rehabilitation techniques to upgrade the joint response using steel and *FRP* jacketing were examined [5-8]. However, analytical studies are limited. A joint element that accounts for the fixed end rotation at the beam-column interface due to bond-slip of the reinforcement steel bars was presented [9]. The model was successful but did not include joint shear effects. Ghobarah and Biddah [10] proposed a joint model consisting of two flexural springs in series. The model oversimplified the bond-slip behaviour. Several analytical studies were carried out on the performance of non-ductile reinforced concrete frames when rehabilitated using

X-steel bracing [11-14]. Steel braces may be installed in reinforced concrete moment resisting frames to provide an alternate lateral load resisting system. Yet, no similar studies for frames rehabilitated with fibre reinforced polymer (*FRP*) composites exist. The objective of this study is to examine and compare the effect of two rehabilitation techniques; *FRP* joint jacketing and *X*-steel bracing on the response of *RC* frames. The analysis takes into account the effect of joint deformation on the global dynamic response of the frames.

2. Design of Existing Frames

Two reinforced concrete moment resisting frame structures, 9-storey and 18-storey, were selected for the analysis. The buildings measured 18*m* by 30*m* in plan, with a bay width of 6*m* (3 bays by 5 bays) and floor height of 3.6*m*. The frames represent typical office buildings that were constructed in accordance to pre-seismic codes [15]. Concrete compressive strength of 21*MPa* and steel yield strength of 300*MPa* were used. Non-ductile reinforcement details in the building include beam bottom longitudinal reinforcement anchored 150*mm* into the joint zone and no transverse reinforcement in the beam-column joints. An interior frame was selected for the analysis. The concrete dimensions and the reinforcement details of the frame elements are shown in Figure (1). The weight due to dead load on the frames was calculated to be 663.5*kN/floor*. The periods of free vibration of the first two modes were determined to be 1.51 and 0.54*s* for the 9-storey frame and 2.67 and 0.96*s* for the 18-storey frame, respectively. A critical damping ratio of 2% was assumed for all the modes of vibration of the two frames regardless of the joint detailing. The mass and stiffness proportional Rayleigh damping approach was used in the analysis.

3. Design of Rehabilitated Frames

Two rehabilitation techniques were proposed. The first technique was applied to eliminate the non-ductile failure modes such as joint shear failure and steel bars bond-slip. Three uni-directional glass fibre reinforced polymer (*GFRP*) sheets were applied to the beam-column joint to account for the missing transverse reinforcement. The properties of the composite sheets are:

Modulus of elasticity = 71*GPa*,

Ultimate strength = 1700*MPa*

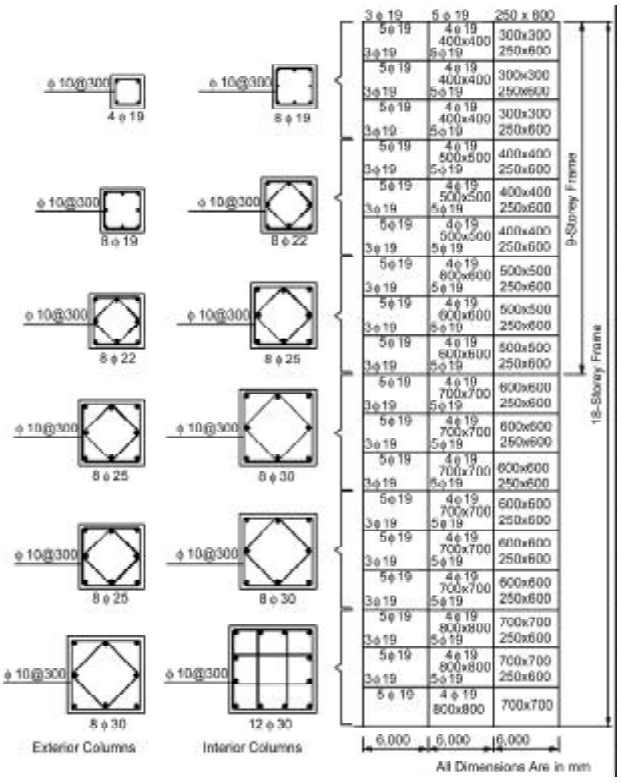

Figure 1. Section dimensions and reinforcement details of the RC frames.

Ultimate strain = 2.0%,

Design thickness = 0.353*mm*

The problems associated with beam bars bond slip and insufficient anchorage of the bottom beam bars in the joint zone, are not included in the model as a possible failure mode. The reason is that it was demonstrated [16] that it is possible to eliminate the bond slip by transferring the beam bars tensile forces using threaded rods to the column by a plate in bearing. The technique significantly improved the ductility and strength of the beam-column joint and can be applied to exterior as well as interior joints.

In the second rehabilitation technique, concentric X-steel bracing was considered in the middle bay along the frame height, as shown in Figure (2). The brace members were selected as round hollow steel section (*HSS* 114 x 8) and were uniformly distributed along the frame height. The brace properties are:

E = 200,000*MPa*, f_y = 350*MPa*, P_c/P_y = 0.415
P_r/P_c = 0.33, r = 37.7*mm*, KL/r = 113

Where E is the modulus of elasticity of steel, f_y is the steel yield strength, P_y is the brace yield force in tension, P_c is the brace capacity in axial compression, P_r is the post-buckling strength, r is the radius of gyration of the cross section, and KL is the effective

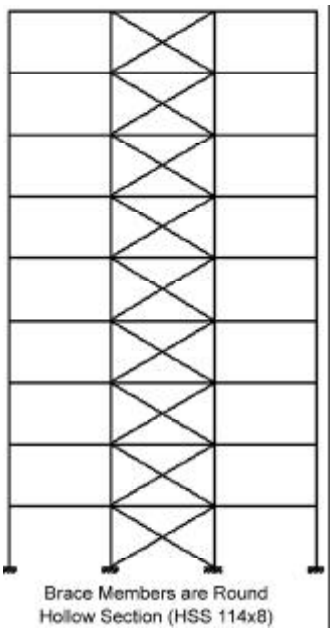

Figure 2. Rehabilitation technique using concentric X-steel bracing.

brace length.

As example, details of a possible connection between the concentric X-bracing and the *RC* frame members are shown in Figure (3). The force in the brace is transferred to the frame using steel plates attached to the concrete columns and beams. The steel plates surrounding the beams are anchored through the concrete section while the steel plates of the column are welded together. The force in the brace member was transferred to the beam and the column plates through a gusset plate [13]. There are other connections that can be considered, however, the analytical model used is not sensitive to the connection details.

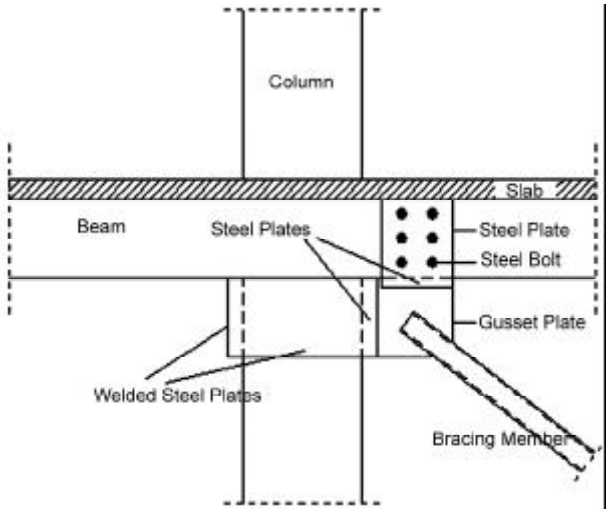

Figure 3. Connection detail of the bracing member to the existing concrete frame elements [13].

The periods of vibration of the concrete frames rehabilitated using steel braces were found to be approximately half those of the frame with flexible joints.

4. Analytical Model

In the analysis, the concept of macromodeling is adopted. The flexural elements are modeled as elastic beam-column element with inelastic concrete and steel springs at their ends to capture the inelastic flexural behaviour. The beam-column joint is represented by four pin-connected rigid elements, which are diagonally connected by two inelastic shear springs.

4.1. Flexural Elements

A multi-spring model of concrete flexural elements was adopted [17]. The flexural member is represented as an elastic beam-column element with five zero-length inelastic springs at the member ends. Each of the four exterior springs represents the stiffness of the effective reinforcing bars and the surrounding concrete in compression. The spring at the centre represents the effective concrete in the central region of the section. The flexural element is represented by an elastic beam-column element with three steel and three concrete springs at each end. The interaction between the steel and the surrounding concrete is included in the steel spring behaviour. The hysteretic model of the steel spring [18] shown in Figure (4), was adopted. The monotonic response of the spring is represented by an initial elastic stiffness K_s to the steel yield force P_{sy}, then a post-yield stiffness rK_s to the steel maximum force P_{su}. To represent the post-slip failure behaviour of the steel spring, the steel force P_s corresponding to steel displacement d_s is:

$$P_s = P_{su}[R_{so} + \frac{1-R_{so}}{1+\alpha_s(d_s-d_{su})^2}] \quad (1)$$

where d_{su} is the steel spring displacement that corresponds to the maximum force in the spring.

R_{so} is the ratio between the residual and maximum force in the spring.

α_s is the softening factor.

The effective area of the exterior concrete spring, A_{ce} is determined as the compression zone at ultimate moment. The effective area of the central

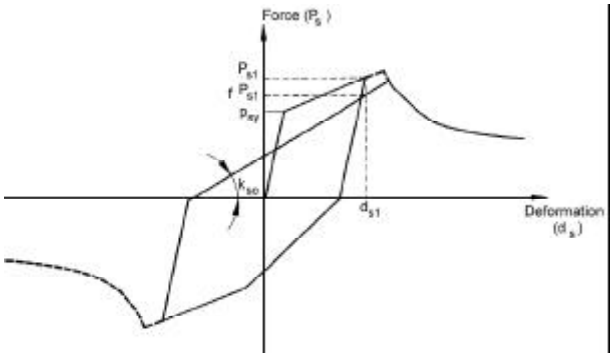

Figure 4. Hysteretic model for steel spring [18].

spring, A_{ci} is written as:

$$A_{ci} = A_g - 2A_{ce} - \sum A_{st} \quad (2)$$

where A_g is the gross cross-sectional area.

$\sum A_{st}$ is the sum of steel bars cross-sectional areas.

The yield force of the concrete spring, P_{cy} that corresponds to concrete ultimate stress, equals:

$$P_{cy} = 0.85 k_h A_c f_c^{'} \quad (3)$$

where $A_c = A_{ce}$ for exterior spring, and $A_c = A_{ci}$ for interior spring.

k_h is the confinement coefficient $= \frac{f_{cc}^{'}}{f_c^{'}}$, where $f_{cc}^{'}$ and $f_c^{'}$ are the confined and unconfined concrete strengths, respectively.

The plastic deformation of the effective concrete element is postulated to represent the accumulated crushing behaviour of the concrete over the plastic hinge length. The concrete spring yield displacement d_{cy} that corresponds to the spring yield force is determined as the integration of the strain at ultimate condition over the member length. The hysteretic model of the concrete springs [18] shown in Figure (5), was adopted. A parabola represents the monotonic response of the concrete spring in compression until the spring yield force is reached. A straight line represents the post yield response. The spacing between exterior springs is determined such that the inelastic springs produce the same yield moment of the original section.

4.2. Beam-Column Joints

The kinematic joint model proposed by Youssef and Ghobarah [18,19] was adopted. In this model, the joint core is represented by four rigid pin-connected elements Two diagonal shear springs connect the corners of the joint core. During the analysis, the joint shear force-shear deformation relationship is predicted. The force in each of the diagonal springs, F can be calculated from simple equilibrium as:

$$F = \frac{V_j}{2\cos\phi} \quad (4)$$

where V_j is the joint shear force, and ϕ is the spring inclination.

The deformation of the spring can be estimated from the joint shear rotation using simple geometry. The hysteretic response of the shear springs is shown in Figure (6).

Modeling of the *FRP* jacket took into account the increased confinement effect on the concrete strength and the shear force resistance of the fibres that cross the shear cracks.

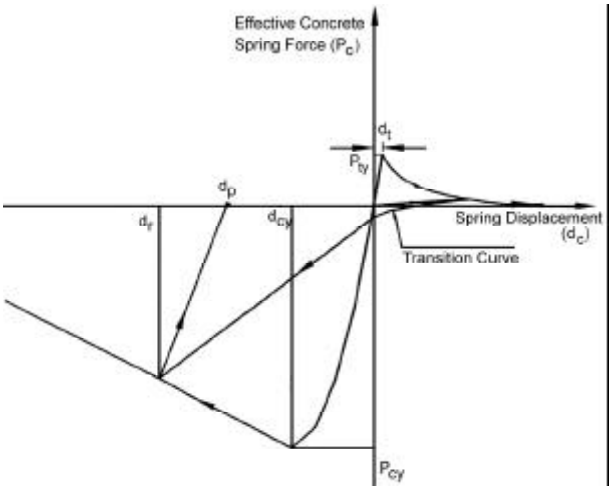

Figure 5. Hysteretic response for concrete spring [18].

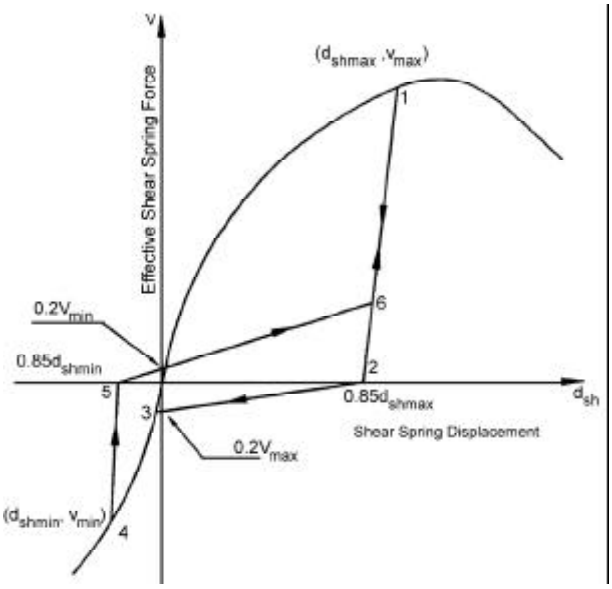

Figure 6. Hysteretic response for shear spring [18].

4.3. Steel Brace Model

Several models have been developed to represent the inelastic hysteretic behaviour of steel brace members. These models include finite element models [20] and macro models [21,22]. In the current study, the Jain and Goel model [23] shown in Figure (7) was selected for its simplicity to represent the buckling behaviour of steel braces.

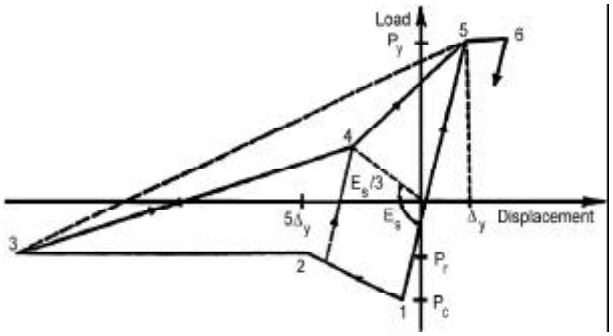

Figure 7. Hysteretic model of steel bracing members [23].

In this Figure, P_y and Δ_y represent the yield strength and displacement of the brace in tension, P_c represents the buckling load under monotonic loading and it can be reached once during the entire loading history. The post buckling response is represented by negative stiffness (segment 1-2) until the residual post-buckling capacity P_r at a compression displacement equals five times the yield displacement, is reached. The built-in brace element in the computer program *PC-ANSR* [24] was used to represent the brace members after appropriate selection of the element parameters to reduce its general hysteretic model to the Jain and Goel model.

4.4. Verification Example

In order to evaluate the proposed modeling approach, the experimental response of a 2-storey concrete frame [25,26] was compared to the analytical prediction. Shake table test of half-scale concrete frame was performed. The frame consisted of two bays 2.50*m* wide and 1.50*m* high. The exterior columns width and depth were 130 and 170*mm*, respectively, whereas the interior columns width and depth were 130 and 180*mm*, respectively. All columns were reinforced using 4 # 10 longitudinal bars (nominal diameter 11.3*mm*). The width and depth of the beams at first floor were 150 and 160*mm*, respectively, whereas the beams at the roof had a width of 140*mm* and a depth of 150*mm*. The *N*04*W* component of the accelerogram recorded in Olympia, Washington, during the April 13, 1949, Western Washington earthquake was chosen as the base motion input for the shake table test. The record was scaled to a peak horizontal ground acceleration (*PGA*) of 0.42*g*. Figure (8a) shows the roof displacement time history as recorded from the shake table test versus the analytical prediction using *RUAUMOKO* software. Figure (8b) shows the analytical prediction of the roof displacement using the adopted modeling technique in the current study. It was found that the proposed modeling technique agrees well with the experimental results in terms of the predicted roof displacement, however, it overestimated the response frequency.

5. Frame Response

The dynamic time history analyses of the 9-storey and 18-storey frames were performed using a modified version of the computer program *PC-ANSR*. The masses are lumped at the beam-column joints. The

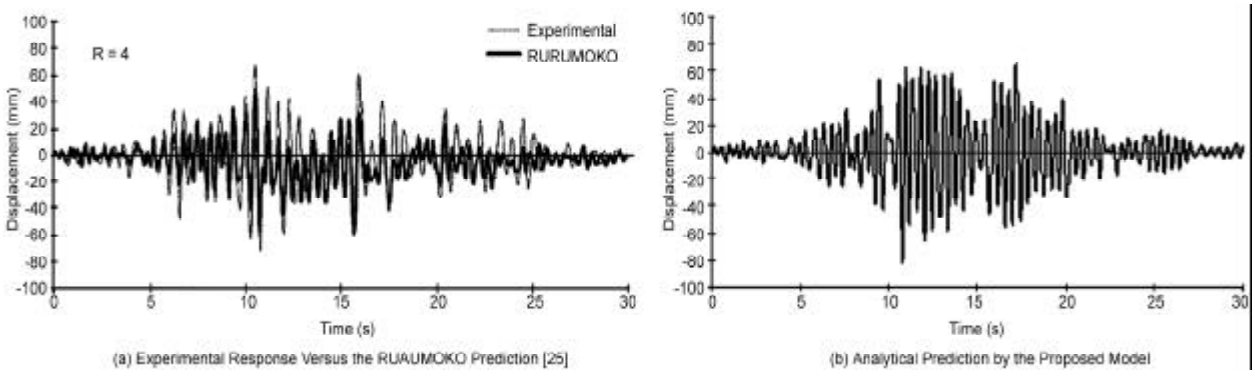

Figure 8. Roof displacement time history of two storey concrete frame.

dynamic analysis of the building when subjected to ground motion was carried out by solving the equation of motion using step by step Newmark-Beta integration procedure. Integration time step of 0.001*s* was used. The *S*00*E* component of *El* Centro record of the 1940 Imperial Valley earthquake, California was selected as input ground excitation after being scaled to different *PGA* values.

5.1. The 9-Storey Frame

Figure (9) compares the roof displacement time history of the 9-storey frames, when subjected to the ground motion scaled to *PGA* levels of 0.2*g* to 0.4*g*. The maximum roof displacements during the loading history are listed in Table (1). From the table, it is observed that even with significant inelastic action occurring at the highest ground acceleration level the resulting displacements are approximately proportional to the levels of acceleration. It is observed that at different ground motion levels, the steel bracing significantly reduced the roof displacement to about 30% of the displacement of the frame with flexible joint assumption. It was also observed that the *FRP* rehabilitation technique did not significantly alter the roof displacement response. During the first 10 second of the loading history, the response of the existing frame with flexible joint assumption was very similar to that of rigid joint assumption and that rehabilitated using

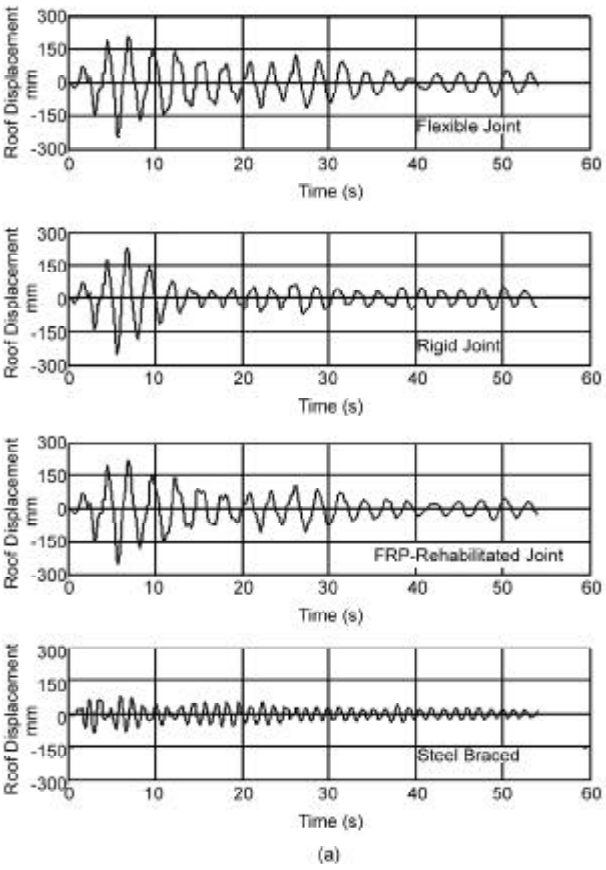

Figure 9a. Roof displacement response of 9-storey frames when subjected to El Centro scaled to 0.2g.

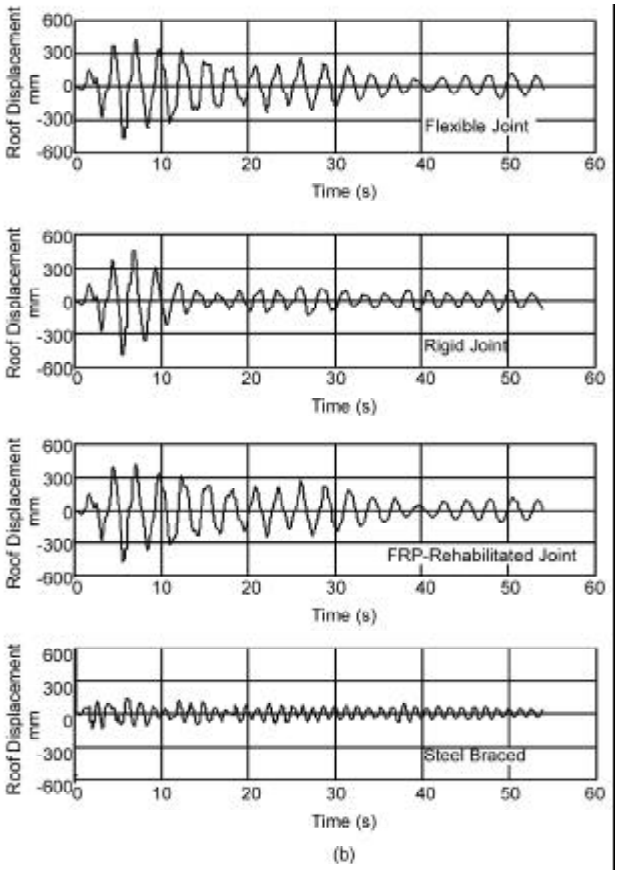

Figure 9b. Roof displacement response of 9-storey frames when subjected to El Centro scaled to 0.4g.

Table 1. Response of the 9-storey frames.

Frame Model	Maximum Roof Displacement for Various PGA Levels (mm)				Maximum Interstorey Drift for Various PGA Levels (%)			
	0.1g	0.2g	0.3g	0.4g	0.1g	0.2g	0.3 g	0.4 g
Flexible Joint Frame	128.5	244.9	357.2	480.1	0.62	1.17	1.71	2.27
Rigid Joint Frame	123.8	250.3	376.9	502.5	0.53	1.21	1.80	2.41
FRP-Rehabilitated Frame	130.1	252.3	368.4	481.7	0.63	1.20	1.81	2.24
Steel Braced Frame	37.9	85.5	123.3	138.4	0.22	0.34	0.44	0.64

FRP composites. Following this, the deflection of the frame with rigid joint assumption was much lower than the other two frames due to the damage in the joint zone of the existing frame and the concrete crushing of some flexural elements in the *FPR*-rehabilitated frame.

The envelopes of lateral displacement for the 9-storey frames at maximum roof displacement are shown in Figure (10). The response of the flexible joint frame and *FRP*-rehabilitated joint frame almost coincide. This is because the *FRP* jacket does not change the frame stiffness significantly. The rigid frame experienced slightly more deflection than the flexible and the *FRP*-rehabilitated frames at different *PGA* levels. This is because the frequencies of free vibration of the frame with flexible joint assumption are low when compared with the frequency content of the selected ground motion. The lateral deflection profile of the frame with X-steel braces reflects the high rigidity of the frame and the predominance of the first mode of vibration.

Figure (11) shows the maximum interstorey drift at each storey level of the 9-storey frames. The frame with steel bracing showed almost equal interstorey

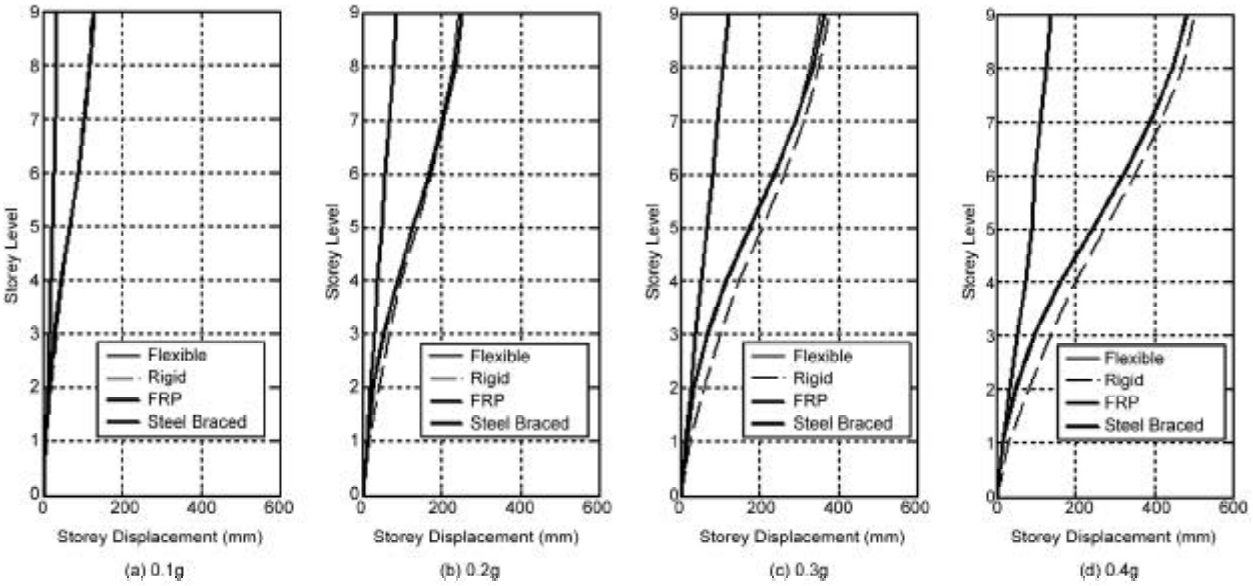

Figure 10. Deflected shape of the 9-storey frames at maximum roof displacement when subjected to ground motion of different PGA levels.

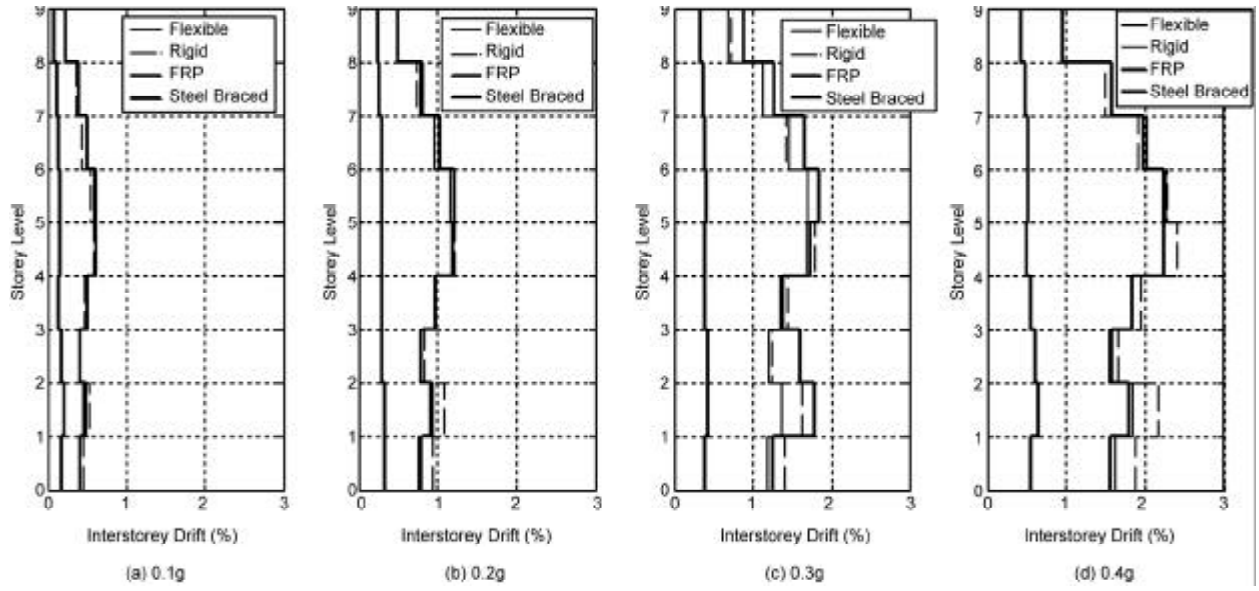

Figure 11. Maximum interstorey drift of the 9-storey frames due to El Centro earthquake.

drift at different storey levels regardless of the level of ground motion. The maximum interstorey drift for the frame with rigid joint assumption occurred at the fifth and the sixth storey levels due to concrete crushing of some beams as shown in Figure (12). The maximum interstorey drift for the frame rehabilitated using *FRP* composites was found to occur in the second, fifth and sixth storey levels where concrete crushing of some exterior column and exterior beams took place as shown in Figure (12). The frame with flexible joint assumption experienced a maximum interstorey drift level of 2.27% at a ground excitation of 0.4*g*, which exceeds the limit of 2% that is recommended by the National Building Code of Canada [27] to control damage and avoid structural instability. The steel braces reduced the maximum interstorey drift to 0.64% at a ground excitation level of 0.4*g*, which is 28% of interstorey drift experienced by the existing frame.

Shear failure of the interior joints of the flexible frame occurred at the first six storeys then progressed to the top three storeys with increasing ground motion level, as shown in Figure (12). When using *FRP* jackets to strengthen the joint shear capacity, joint shear failure was eliminated and concrete crushing in some columns and beams occurred. The frame rehabilitated using steel braces experienced some damage in exterior joints with some concrete crushing in the top storey columns. In general, the rehabilitated frames using *FRP* composites or steel braces showed more controlled damage pattern than that of the existing frame.

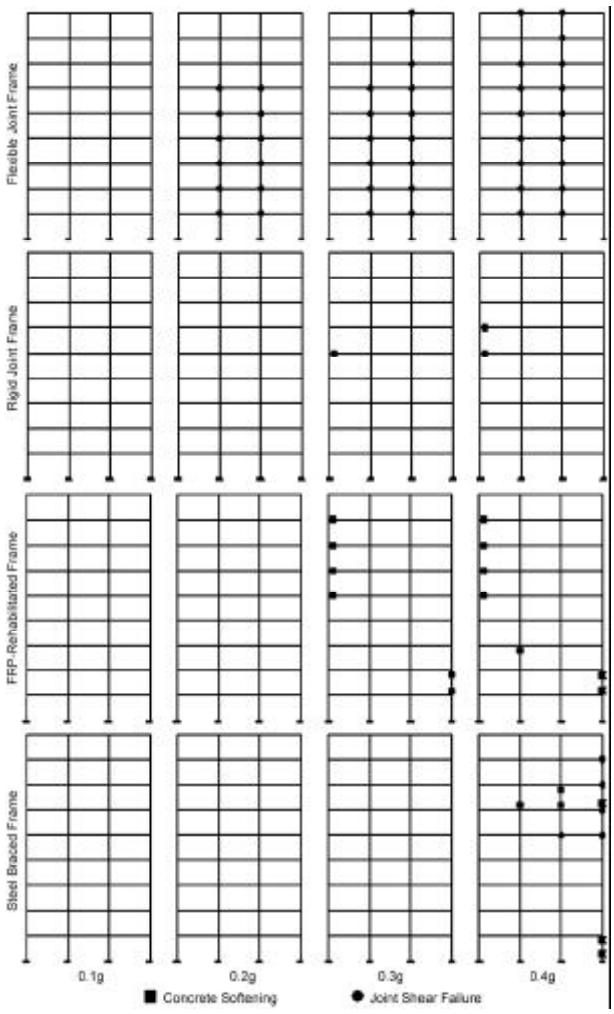

Figure 12. Damage pattern for the 9-storey frames.

5.2. The 18-Storey Frame

Figure (13) compares the roof displacement time history response for the 18-storey frames. Table (2) summarizes the results of the maximum roof displacement and interstorey drift of these frames. When comparing the performance of a frame with flexible joint assumption to that of rigid joint assumption, the characteristics of the ground motion have significant effect on the results. A flexible frame has longer natural period than a rigid frame and therefore it attracts less inertia force when subjected to ground excitation. On the other hand, a flexible frame would have less global stiffness than a rigid frame and thus under the same load level would experience more deflection. Another factor that affects the deflection is when joints are assumed more flexible the frame behaviour approaches that of a flexural beam. Rigid joint assumption causes the frame to behave more like a shear beam. A flexural beam has

Table 2. Response of the 18-storey frames.

Frame Model	Maximum Roof Displacement for Various PGA Levels (mm)				Maximum Interstorey Drift for Various PGA Levels (%)			
	0.1g	0.2g	0.3g	0.4 g	0.1g	0.2g	0.3g	0.4 g
Flexible Joint Frame	110.5	221.0	331.4	442.0	0.65	1.31	1.96	2.61
Rigid Joint Frame	80.8	158.1	245.7	326.6	0.28	0.50	0.86	1.07
FRP-Rehabilitated Frame	81.9	168.2	255.9	343.9	0.26	0.60	0.87	1.16
Steel Braced Frame	118.4	210.0	233.7	275.7	0.30	0.52	0.63	0.72

less displacement at the lower stories than the shear beam and vice versa near the top. Therefore, under seismic load the interstorey drift of the flexible frame is not necessarily greater than that of the rigid frame. The frame with rigid joint assumption experienced more lateral deflection than the frame with flexible joint at different storey levels except the top two storey levels, as shown in Figures (14) and (15). Shear failure of exterior joints of the top stories in the flexible frame occurred, as shown in Figure (16),

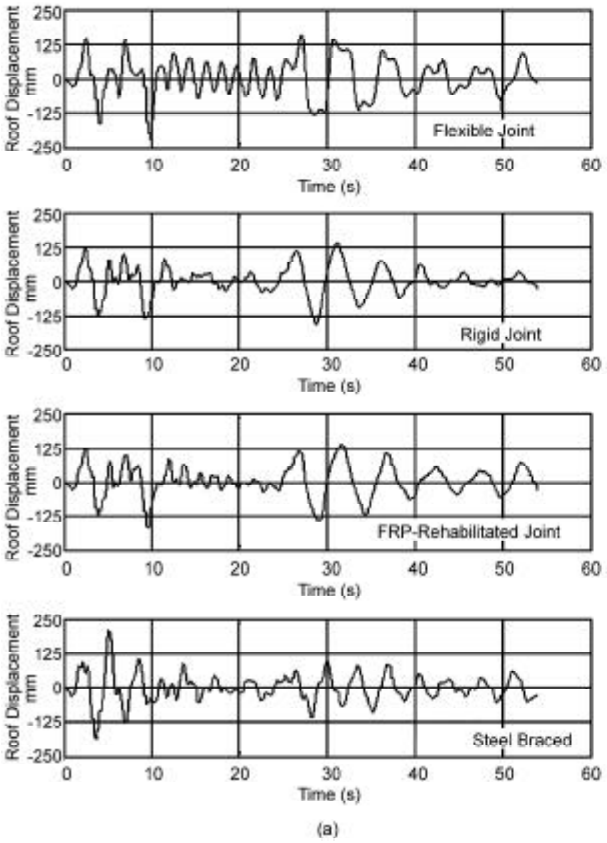

Figure 13a. Roof displacement response of 18-storey frame when subjected to El Centro record scaled to 0.2g.

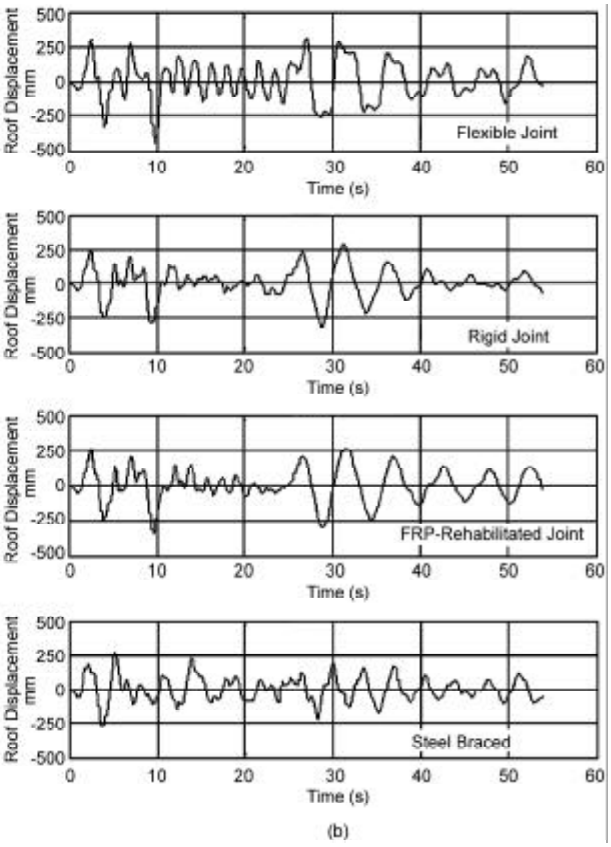

Figure 13b. Roof displacement response of 18-storey frame when subjected to El Centro record scaled to 0.4g.

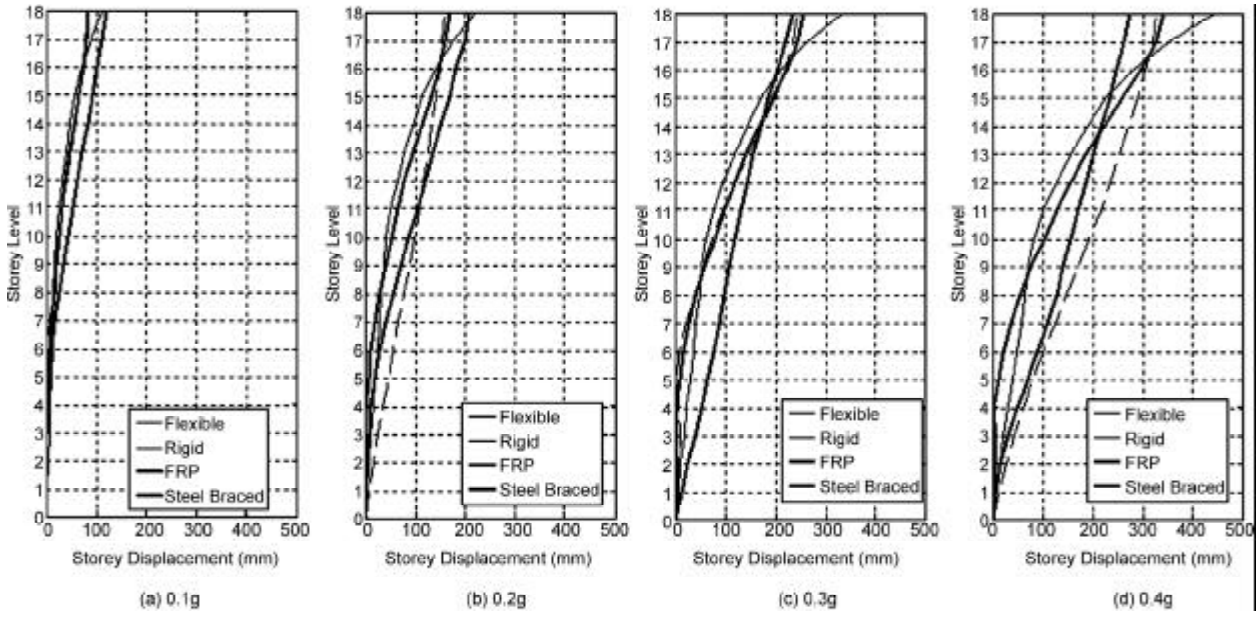

Figure 14. Deflected shape of the 18-storey frames at maximum roof displacement when subjected to ground motion of different PGA levels.

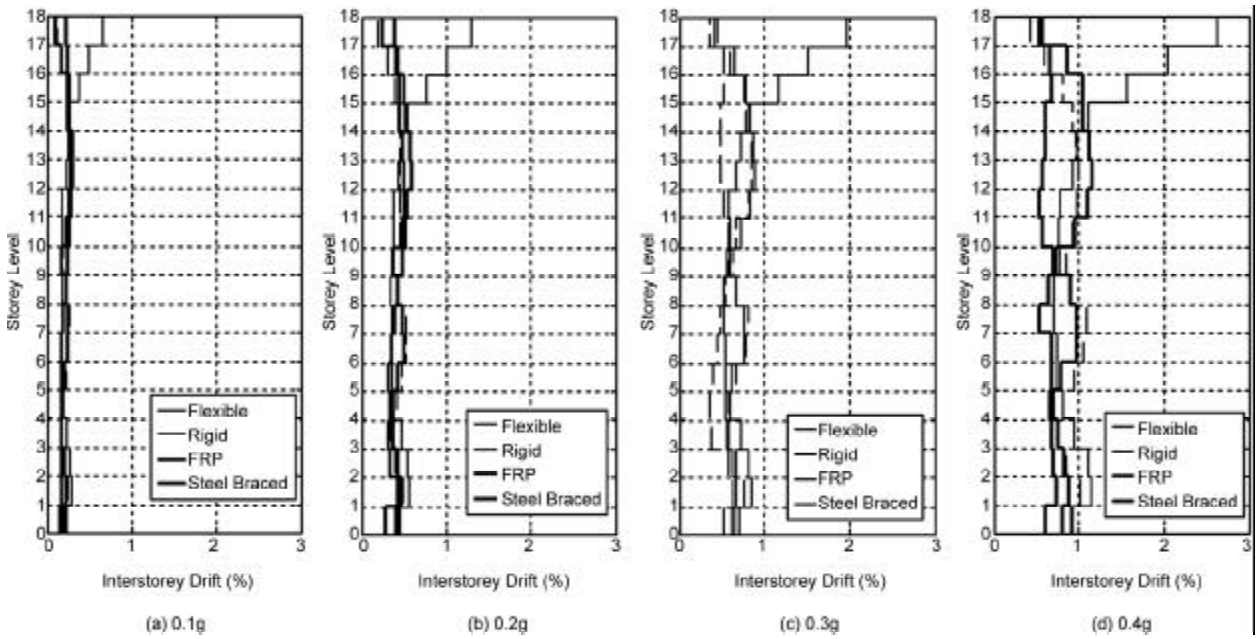

Figure 15. Maximum interstorey drift of the 18-storey frames due to El Centro earthquake.

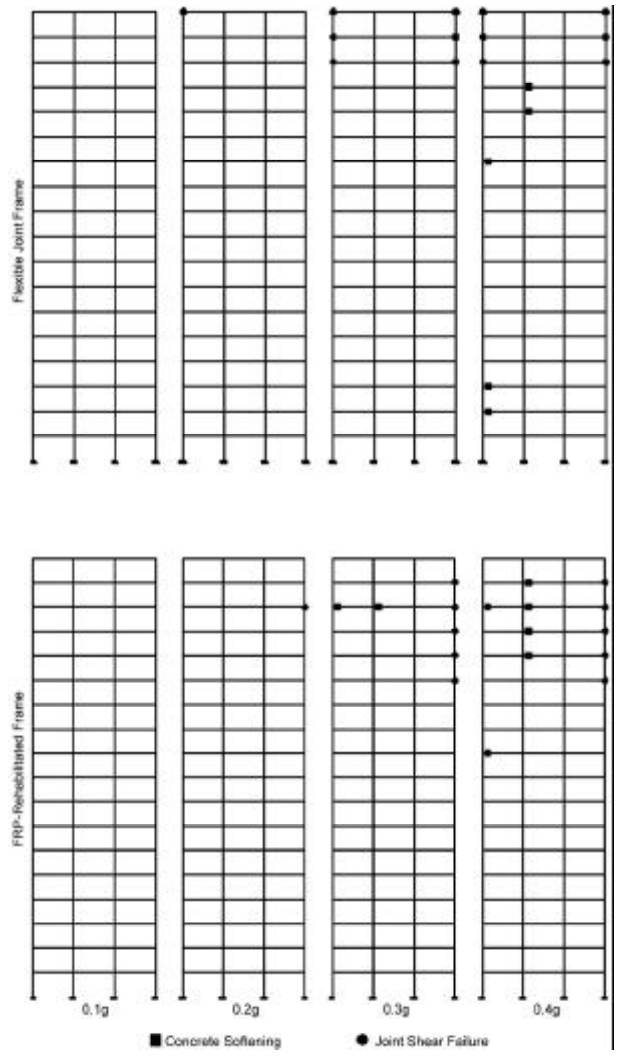

Figure 16. Damage pattern for the 18-storey frames.

and caused excessive lateral deformation to the frame. When comparing the two rehabilitation schemes, the *FPR*-rehabilitated frame experienced less roof deflection than the frame strengthened using steel braces at ground motion level of 0.1*g* and 0.2*g*. However, at peak ground acceleration of 0.3*g*, shear failure of the exterior joints at the fourteenth to the seventeenth storeys of the *FRP* rehabilitated frame caused excessive deflection of the frame as compared to steel braced frame. In general, the roof displacements of the two rehabilitated frames were less than that of the flexible frame. At *PGA* of 0.4*g*, the top storey displacements of the flexible frame, FRP-rehabilitated frame, and the steel braced frame were 442.0, 343.9 and 275.7*mm*, respectively.

Figure (15) shows the maximum interstorey drift at each floor level for the 18-storey frames. The rehabilitated frames experienced a maximum interstorey drift of 0.72% for steel braced frame at the second storey level and 1.16% for *FRP*-rehabilitated frame at the thirteenth storey level. The flexible frame showed an interstorey drift of 2.6% at the roof storey at ground excitation of 0.4*g*. In general, the rehabilitated frames experienced inter-storey drift limits less than that of the existing flexible frames, regardless the ground excitation level. The two rehabilitation schemes significantly improved the dynamic response of the 18-storey frame in terms of lateral deflection, interstorey drift and damage pattern.

6. Conclusions

In this study, the effect of joint deformation on the global dynamic structural response was evaluated. The effect of rehabilitation techniques using *FRP* composites or steel braces on the response was investigated. On the basis of the results obtained from the analysis, the following conclusions are arrived at:

- Assuming rigid joints in the analysis give different damage pattern and interstorey drift than what are obtained when joint deformation is accounted for. Accurate assessment of damage patterns in existing structures is needed for determining the optimum locations for joint strengthening.
- The rehabilitation using *FRP* composites does not significantly alter the dynamic response of the frame. However, *FRP*-strengthening significantly changes the damage location and pattern in the frame. This is because the *FRP* composite materials do not significantly affect the initial stiffness of the concrete members but improves the strength.
- The rehabilitation technique using steel braces is very effective in increasing the frame stiffness by providing alternate stiff lateral load resisting system. However, non-ductile failure pattern such as joint shear failure may occur at some locations.
- An integrated scheme using *FRP* composites and steel braces might be more efficient for reducing the frame lateral deflection and eliminating undesirable non-ductile failure mechanisms.
- Introducing more flexibility to the frame in terms of joint shear deformation does not necessarily result in more lateral deflection of the frame, particularly in the case of high-rise structures with long periods of free vibration. The frame response is highly dependent on the characteristics of ground motion.

It is noted that the results and the conclusions presented in this paper were based on limited analysis performed using one earthquake record scaled to different *PGA* levels. The analysis of frames of various heights using different earthquake records is needed in order to define the range of applicability of the conclusions.

References

1. Saatcioglu, M., Gardner, N.J., and Ghobarah, A. (2001). "1999 Turkey Earthquake Performance of RC Structures", *Concrete International*, **23**(3), 47-56.

2. Blume, J.A., Newmark, N.M., and Corning, L.H. (1961). "Design of Multi-Storey Concrete Buildings for Earthquake Motions", Portland Cement Association, Skokie, Illinois, US.

3. Park, R. and Paulay, T. (1975). "Reinforced Concrete Structures", John Wiley & Sons, New York, US.

4. Liu, A. and Park, R. (2001). "Seismic Behaviour and Retrofit of Pre-1970's As-Built Exterior Beam-Column Joints Reinforced by Plain Round Bars", Bulletin of the New Zealand Society for Earthquake Engineering, **34**(1), 68-81.

5. Alcocer, S.M. and Jirsa, J.O. (1993). "Strength of Reinforced Concrete Frame Connections Rehabilitated by Jacketing, *ACI Structural Journal*, **90**(3), 249-261.

6. Hakuto, S. (1995). "Retrofitting of Reinforced Concrete Moment Resisting Frames", Ph.D. Dissertation, Department of Civil Engineering, University of Canterbury, Christchurch, New Zealand, 390p.

7. Ghobarah, A., Aziz, T.S., and Biddah, A. (1997). "Rehabilitation of Reinforced Concrete Frame Connections Using Corrugated Steel Jacketing", *ACI Structural Journal*, **4**(3), 283-294.

8. El-Amoury, T. and Ghobarah, A. (2002). "Seismic Rehabilitation of Beam-Column Joint Using GFRP Sheets", *Engineering Structures*, **24**(11), 1397-1407.

9. Filippou F.C. and Issa A. (1988). "Nonlinear Analysis of Reinforced Concrete Frames Under Cyclic Load Reversals", Report No. UCB/EERC 88-12, Earthquake Engineering Research Center, University of California, Berkeley, CA, US.

10. Ghobarah, A. and Biddah, A. (1999). "Dynamic Analysis of Reinforced Concrete Frames Including Joint Shear Deformation, *Engineering Structures*, **21**, 971-987.

11. Pincheira, J.A. and Jirsa, J.O. (1995). "Seismic Response of RC Frames Retrofitting With Steel Braces or Walls, *Journal of Structural Engineering, ASCE*, **121**(8), 1225-1235.

12. Bouadi, A., Engelhardt, M.D., Jirsa, J.O., and Kreger, M.E. (1994). "Eccentrically Braced Frames for Strengthening of R/C Building with Short Columns", *Proceeding of the Fifth U.S. National Conference on Earthquake Engineering*, Chicago, Illinois, US, **3**, 617-626.

13. Abou-Elfath, H. and Ghobarah, A. (2000). Behaviour of Reinforced Concrete Frames Rehabilitated with Concentric Steel Bracing", *Canadian Journal of Civil Engineering*, **27**(3), 433-444.

14. Maheri, M.R. and Akbari, R. (2003). "Seismic Behaviour Factor, R, for Steel X-braced and Knee-braced Buildings", *Engineering Structures*, **25**(12), 1505-1513.

15. ACI-318 (1963). "Building Code Requirements for Reinforced Concrete", American Concrete Institute, Detroit, Michigan, US.

16. El-Amoury, T., Arafa, A., and Ghobarah, A. (2003). "Strengthening of Seismically Vulnerable Beam-Column Joints", *Proceedings of Response of Structures to Extreme Loading Conference*, Elsevier, UK, Paper No. 17.

17. Lai, S.S., Will, G.T., and Otani, S. (1984). "Model for Inelastic Biaxial Bending of Concrete Members", *Journal of Structural Engineering, ASCE*, **110**(11), 2563-2584.

18. Youssef, M. and Ghobarah, A. (1999). "Strength Deterioration due to Bond Slip and Concrete Crushing in Modeling of Reinforced Concrete Members", *ACI Structural J.*, **96**(6), 956-966.

19. Youssef, M. and Ghobarah, A. (2001). "Modeling of RC Beam-Column Joints and Structural Walls", *Journal of Earthquake Engineering*, **5**(1), 93-111.

20. Fujimoto, M., Wada, A., Shibata, K., and Kosugi, R. (1973). "Nonlinear Analysis of K-Type Braced Steel Frames", Transactions of the Architectural Institute of Japan, No. 209.

21. Roeder, C.W. and Popov, E.P. (1977). "Inelastic Behaviour of Eccentrically Braced Frames Under Cyclic Loading", Report No. EERC 77-18, Earthquake Engineering Research Center, University of California, Berkeley, California, US.

22. Remennikov, A. and Walpole, W. (1995). "Incremental Model for Predicting the Inelastic Hysteretic Behaviour of Steel Bracing Members", Research Report 95-6, Department of Civil Engineering, University of Canterbury, Christchurch, New Zealand.

23. Jain, A.K. and Goel, S.C. (1978). "Hysteretic Models for Steel Members Subjected to Cyclic Buckling", Report No. UMEE 78R6, Department of Civil Engineering, University of Michigan, Ann Arbor, Michigan, US.

24. Maison, B.F. (1992). "PC-ANSR: A Computer Program for Nonlinear Structural Analysis", University of California, Berkeley, CA, US.

25. Filiatrault, A., Lachapelle, E., and Lamontagne, P. (1998). "Seismic Performance of Ductile and Nominally Ductile Reinforced Concrete Moment Resisting Frames, I Experimental Study", *Canadian Journal of Civil Engineering*, **25**, 331-341.

26. Filiatrault, A., Lachapelle, E., and Lamontagne, P. (1998). "Seismic Performance of Ductile and Nominally Ductile Reinforced Concrete Moment Resisting Frames, II Analytical Study", *Canadian Journal of Civil Engineering*, **25**, 342-352.

27. NBCC (1995). "National Building Code of Canada", *The National Research Council of Canada*, Ottawa, Ontario, Canada.